CHAPTER II

THEORY

2.1 Mesoporous Materials

Mesoporous materials are typically amorphous or paracrystalline solids, e.g. silica, transitional alumina, modified layered materials. The pores of these materials are irregularly in spaced and broadly distributed in size. Despite of these efforts, mesoporous molecular sieves with regular, well-defined channel systems have remained elusive.

2.1.1 MCM-41

In 1992 researchers at Mobil Research and Development Corporation announced a new group of mesoporous materials, designated M41S.[2,3] These materials are characterized by narrow pore size distributions, turnable from 1.5 to 10.0 nm, break past the pore size constraint (<1.5 nm) of microporous zeolites. The extremely high surface areas (>1000 m^2/g) and the precise tuning of pore sizes are among the many desirable properties that make such materials the great interest. Main groups of this family are MCM-41, MCM-48, and MCM-50. MCM-48 has a three-dimensional, cubic-ordered pore structure. MCM-41 has a one-dimensional, hexagonally ordered pore structure, and MCM-50 has an unstable lamellar structure. Figure 2.1 shows three

structures of these phases. These materials are fundamentally different from zeolites by the fact that the pore walls are amorphous.

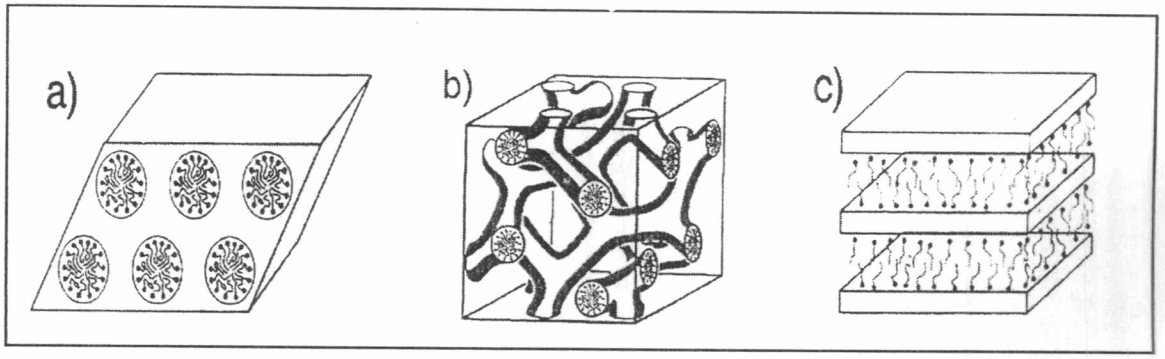

Figure 2.1 A schematic presentation of three inorganic surfactant mesostructures: (A) the hexagonal phase, (B) the cubic phase, and (C) the lamellar phase.

MCM-41 is a member of mesoporous molecular sieves, which possesses a hexagonal array of uniform mesopores as shown in Figure 2.2. It has uniform channels varying from approximately 1.5 to 10.0 nm in size. The larger pore materials typically have surface areas above 1000-m^2/g and hydrocarbon sorption capacities of 0.7 cm^3/g and greater.

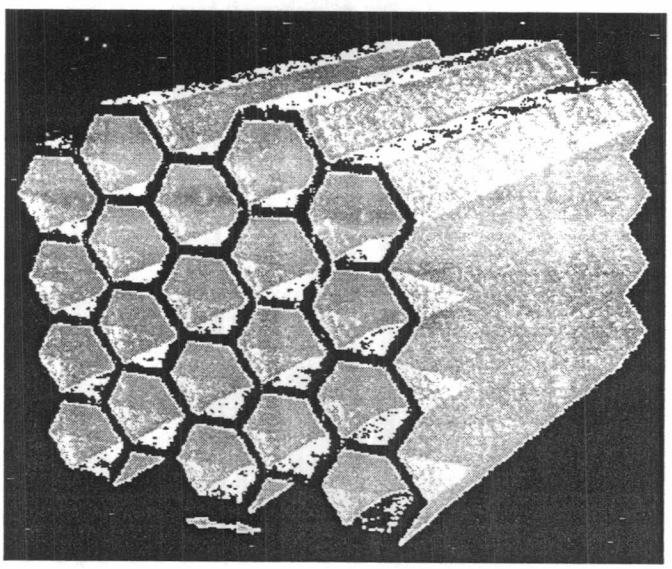

Figure 2.2 Hexagonal packing of unidimensional cylindrical pores.

2.1.2 Synthesis of MCM-41

As traditional zeolite and molecular sieve syntheses, MCM-41 is also prepared by mixing organic surfactants, silica, and silica-alumina source to form a supersaturated solution. The mixture is maintained for crystallization at temperature between 70 and 150 °C for a period of time. The possible routes for obtaining hexagonal mesoporous MCM-41 are summarized in Table 2.1. The pore sizes and interlayer distances of the materials can be tailored by changing the chain length of alkylhexadecyldimethylammonium $[(C_{16}H_{33})(C_nH_{2n+1})(CH_3)_2N^+]$ [59] The longer the chain length is, the larger the pore sizes obtain. Besides, the d_{100} spacing of hexagonal MCM-41 increases with increasing carbon number (n) at the rate of 0.25 nm /C atom.

Table 2.1 Four possible routes for generating mesophase

route	typical examples	pH	resulting phase
S^+I^-	CTA + silicate species	<7 or 10-13	hexagonal, cubic, and lamellar
S^-I^+	$C_{16}H_{33}SO_3^-$ + lead oxide		hexagonal
	$C_{12}H_{25}PO_4^{2-}$ + ion oxide	1-5	lamellar
$S^+H^-I^+$	CTABr + silicate species	<2	hexagonal
	CTABr + zincophosphate	<3	lamellar
S^0I^0	$C_{12}H_{25}NH_2 + (C_2H_5O)_4Si$	<7	hexagonal

S = surfactant ions

I = inorganic species

H^- = anionic halides

For highly ordered MCM-41 structure, acetic acid is added to the reaction system in order to shift equilibrium between reactants and mesophases towards the desired direction. The addition of acid to the gel mixture can be neutralized hydroxides and shift the equilibrium to the positive direction. Therefore, the rate of silica condensation is increased. The brønsted acid sites from the tetrahedrally coordinated Al are the active focus for most hydrocarbon reactions. The most active aluminum source for Al-MCM-41 is sodium aluminate.[14,60] When sodium aluminate was used, all alumunium in the product were 6-coordination. 4-coordinate alumina in MCM-41 framework can only be obtained from aluminium sulfate as aluminum source.[61]Other elements can also generate a new hybrid atom molecular sieve with interesting catalytic properties, especially Ti-MCM-41. Ti-MCM-41 gains much attention as oxidation catalysts because its pore size is large enough to allow most organic reactants, intermediates, and products easily to pass in and out.

2.1.3 Behavior of Surfactant Molecules in an Aqueous Solution

Surfactant molecules manifest themselves as active components with variable structures regarding to their concentrations, as shown in Figure 2.3. At low concentration, they energetically exist as monomolecules. When the concentration increases, the molecules aggregate together to form micelles in order to decrease the system entropy. The initial which surfactant molecules aggregate and form micelles is called "Critical Micellization Concentration" (CMC). As the process continues, hexagonal close packed arrays appear and produce hexagonal phases. The next step is an appearance of cubic phase and lamellar phase. A particular phase in the surfactant aqueous solution at a specific concentration depends not only on concentrations, but also on the nature of itself and environmental parameters, e.g. hydrophobic chainlength, hydrophilic head group, counter ion, pH, temperature, and ionic strength in the solution.[62,63]

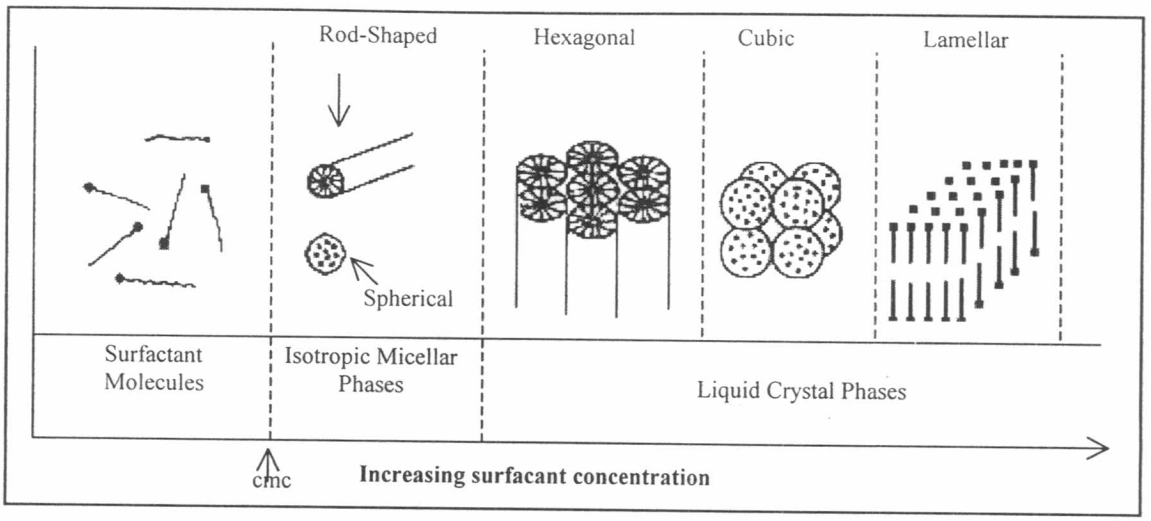

Figure 2.3 Phase sequence of the surfactant-water binary system

2.1.4 Chemistry of Silicates in Alkaline Aqueous Solution

Silicate structures, which are important for molecular sieves synthesis in an alkaline solution, are divided into 25 forms as shown in Figure 2.4.[64] The distribution of these species are sensitive to pH, temperature, cation, and silica concentration. A reduction of silicon concentration, an increase in temperature or pH are favored the formation of monomer and small oligomers.[65] When the ratio of SiO_2/Na_2O is greater than 1, the major form of silica is the connection of Q^3 $[Si(OSi)_3OH]$ and Q^2 $[Si(Osi)_2(OH)_2]$. Small anions, such as cyclic trimer, are found at high silica concentration instead of larger anions.[66]

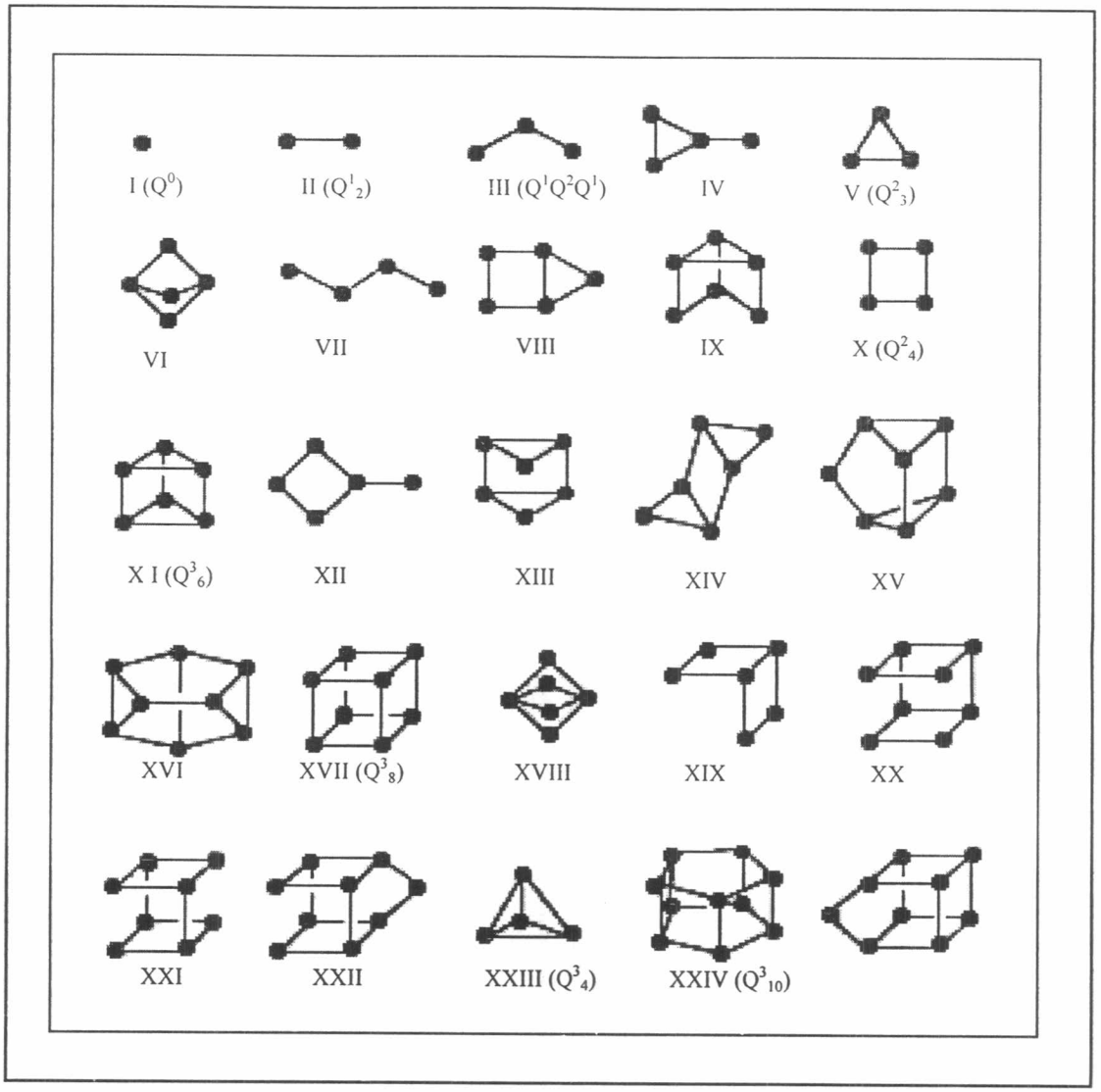

Figure 2.4 Silicate species identified by ^{29}Si NMR in alkaline aqueous solution. Filled circles represent tetrahedral Si atoms; lines represent Si atoms linked through oxygen atom.

2.2 Formation Mechanism

2.2.1 Liquid Crystal Templating Mechanism (LCT)

Beck *et al.* (1992)[2] proposed a mechanism explaining formation of mesoporous structure called Liquid Crystal Templating Mechanism (LCT). The mechanism explains that silicate condensation is not a dominant factor in the formation of mesoporous structure, but the whole process of two possible pathways is included as shown in Figure 2.5. For pathway 1, hexagonal crystal mesophases form prior to addition of silicate species. While for pathway 2, the silicate species added to the reaction mixture influence the order of isotropic rod like micelles of the desired liquid crystal phase, i.e. hexagonal mesophase. Therefore, the mesophase is structurally and morphologically directed by the existence of liquid crystal micelles and mesophases.

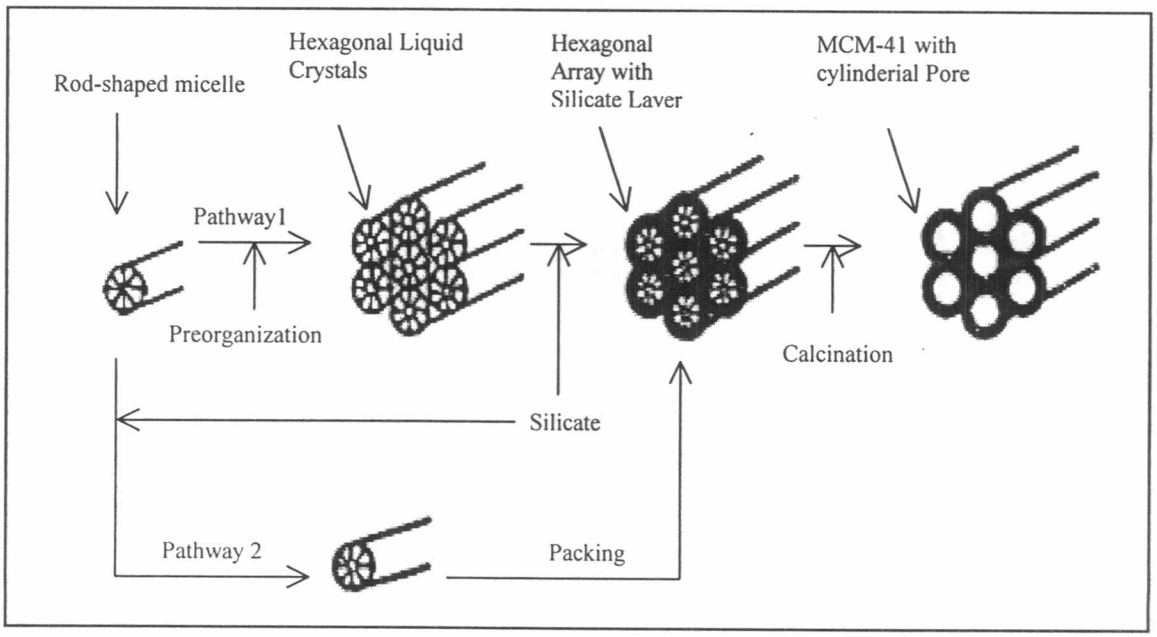

Figure 2.5 Schematic model of liquid crystal templating mechanism via two possible pathways

The effect of surfactant/silica molar ratio was recognized. When the surfactant/silica molar ratio increased from 0.5 to 2.0, the obtained siliceous products were classified into four separate groups: MCM-41 (hexagonal), MCM-48 (cubic), thermally unstable lamellar phase, and cubic octamer $[(CTMA)SiO_{2.5}]_8$. The data are in excellent agreement with the behavior of surfactants in solution as shown in Figure 2.3. The influence of alkyl chain length (C_6-C_{16}) and reaction temperatures (100-200 °C) on the resulting products was also extensively investigated.[15] Figure 2.6 shows the XRD patterns of synthesized products with different surfactants and temperatures. At 100 °C, the products are in the sequence of amorphous materials, poorly defined MCM-41, and well defined MCM-41, respectively, when the alkyl chain is increased. At 150 °C, ZSM-5 zeolite with high crystallinity is generated from both C_6 and C_8 surfactants. The product using C_{10} surfactant is less defined, comparing with others using C_{12}, C_{14} and C_{16} surfactant. At 200 °C, ZSM-5 is synthesized from C_6. A mixture of ZSM-5, ZSM-48, and dense phase is from C_8-C_{14}, and amorphous phase is from C_{16}.

2.2.2 Transformation Mechanism from Lamellar to Hexagonal Phase

A micellar assembly of organic molecules is broken up and rearranged upon addition of inorganic species, in order to form a new phase with lamellar morphologies. A lamellar phase is indeed isolated between the reaction periods of 1-20 min at 75 °C. After 20 min, the hexagonal phase is simultaneously detected as shown in Figure 2.7[18,19]. When the lamellar phase is hydrothermally treated at 100 °C, it converts to the hexagonal phase over 10 days with an intermediate.

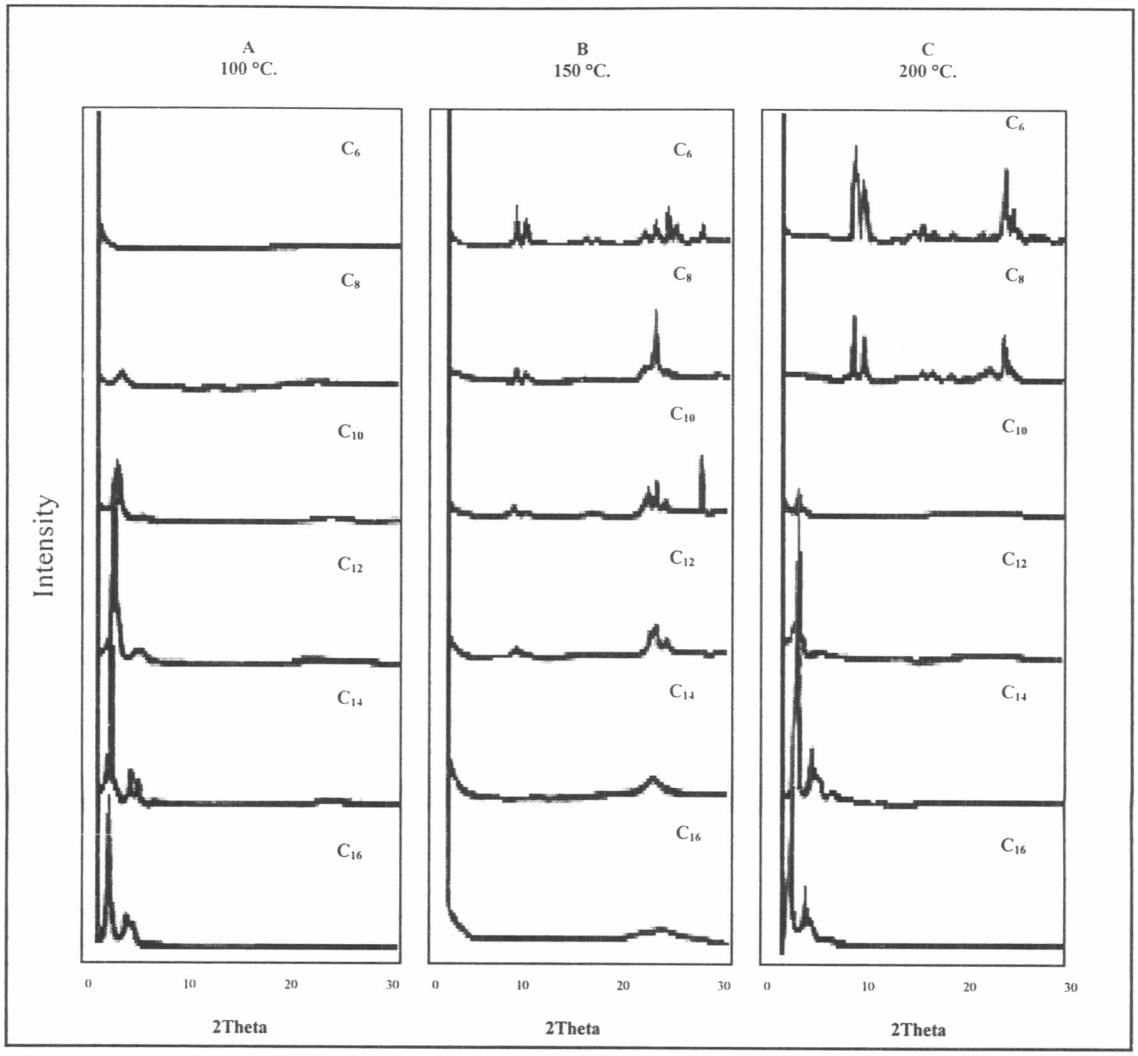

Figure 2.6 X-ray powder diffraction patterns of calcined products obtained using different surfactant at various temperature: 100 °C (A) 150 °C (B) 200 °C (C)

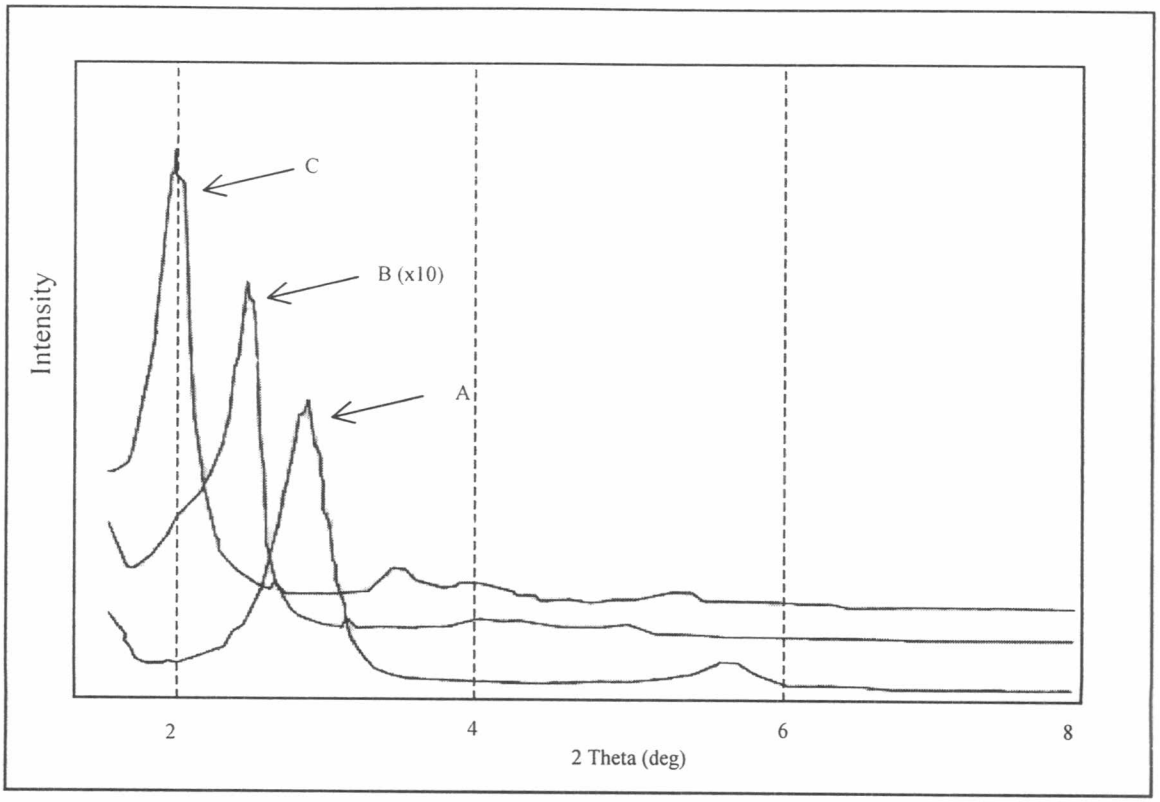

Figure 2.7 X-ray powder diffraction patterns of (A) the initially lamellar phase, (B) an intermediate material of A after hydrothermal treatment, and (C) the hexagonal phase transformed from A after hydrothermal treatment for 10 days

2.3 Characterization and Physicochemical Properties

2.3.1 X-ray Diffraction (XRD)

When mesoporous molecular sieves are synthesized, many experimental techniques are used to characterize properties. XRD is a powerful technique providing direct information of pore architecture. For mesoporous molecular sieves, diffraction patterns are in the low angle range, 2θ less than 10 degree. No reflections are observed at higher angles; thereby, it has been concluded that the pore walls are mainly amorphous. The order of lines can be indexed according to lattice planes. However, XRD powder diffraction data is not only used as a

"fingerprint" for the identifying of the pore structure, but other information can also be exploited as summarized in Table 2.2.

Table 2.2 XRD powder diffraction information

Feature	Information
Peak positions (2θ values)	Unit cell dimensions
Non-indexable lines	Presence of a crystalline impurity
Systematicallly absent reflections	Symmetry
Background	Presence (or absence) of amorphous material
Width of peaks	Crystallite (domain) size
	Stresss/strain
	Stacking faults
Peak intensities	Crystal structure

The XRD pattern of MCM-41 typically shows three to five reflections of 2theta (2θ) between 2° and 5°. The reflections are due to the ordered hexagonal array of parallel silica tubes. They can be indexed assuming a hexagonal unit cell as (100), (110), (200), (210), and (300), respectively. Since the materials are not completely crystalline at the atomic level, no reflections at higher angles are observed. When an X-ray beam strikes a crystal surface at a specific angle, a portion of the beam is scattered by the layer of atoms at the surface as shown in Figure 2.8. The unscattered portion of the beam penetrates to the second layer of atoms, where d is the interplanar distance of the crystal. Thus, constructive interference of the beam at angle θ is designed by the Bragg equation.

$$n\lambda = 2d \sin\theta \quad \text{.....Bragg Equation}$$

For a hexagonal structure, the characteristics of d-spacing ratio are given as following.

$$d_{100}/d_{110} = d_{200}/d_{220} = 1.732$$

$$d_{100}/d_{200} = d_{200}/d_{400} = 2.000$$

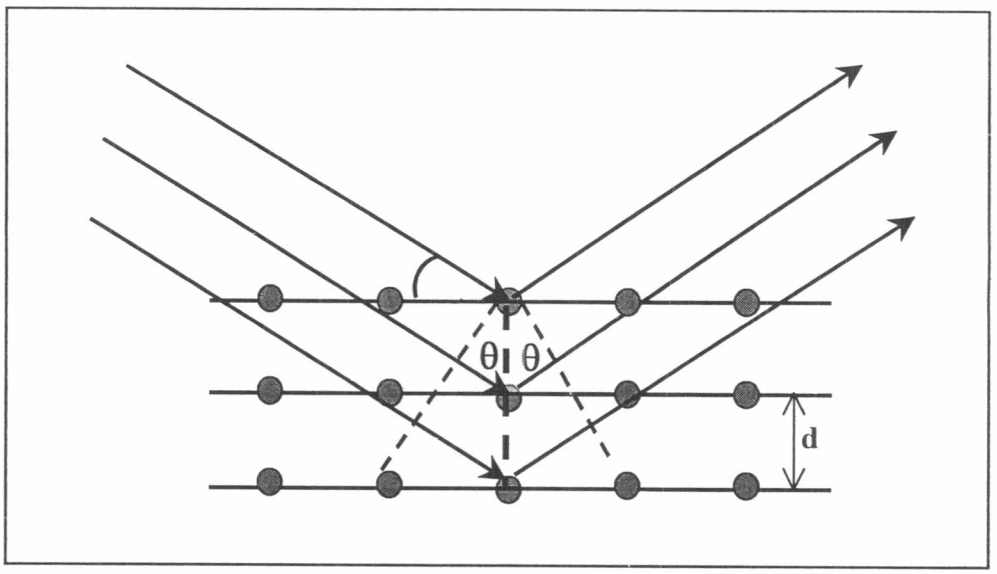

Figure 2.8 Diffraction of X-rays by a crystal.

2.3.2 BET Surface Area

Nitrogen adsorption-desorption techniques are commonly used for determining porosity and BET surface area of the materials. The BET surface area of MCM-41 is higher than 1,000 m^2/g, and pore size distribution has been calculated using BJH program. The most common adsorbate is probably N_2 at 77 K. According to the IUPAC definition, mesoporous materials exhibit a Type IV adsorption-desorption isotherm as shown in Figure 2.9. At low relative pressures (p/p_0), adsorption only occurs as a thin layer on the wall (monolayer coverage). After that, a sharp increase is seen at relative pressures from 0.25 to 0.5, depending on pore size. That corresponds to the capillary condensation of N_2 in the mesopores. The sharpness of the inflection reflects uniformity of pores and height indicates pore volume.

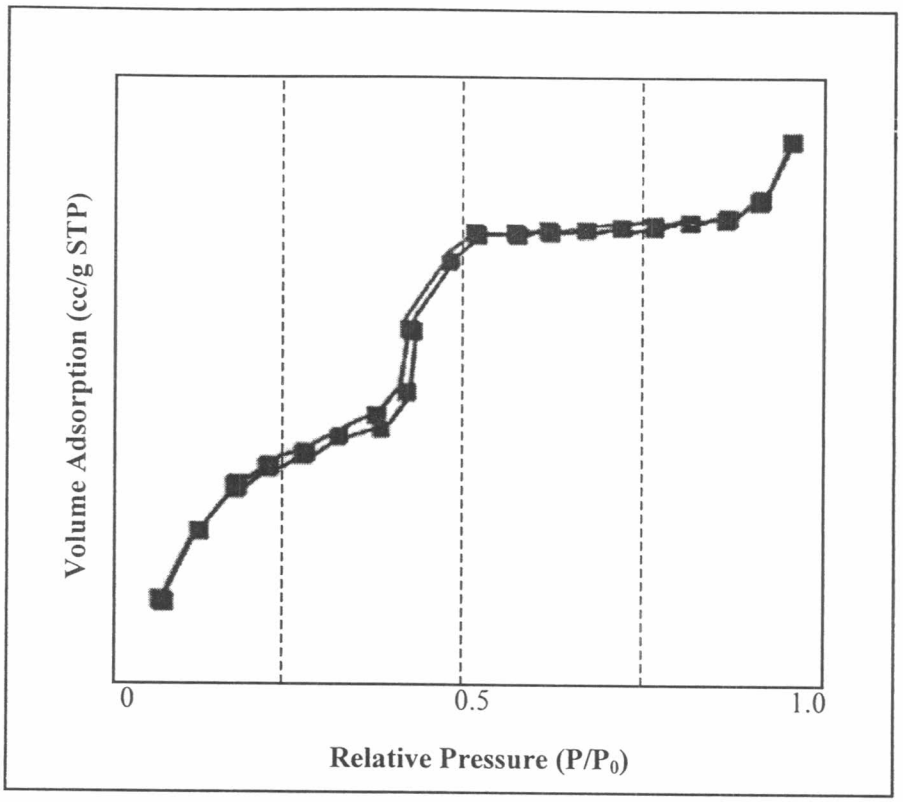

Figure 2.9 N_2 adsorption-desorption isotherms of MCM-41

2.3.3 Stability

MCM-41 is thermally stable, but the hydrothermal stability is poor, as represented in Table 2.3. Calcination of MCM-41 in dry air resulted in slight loss of BET surface area. When MCM-41 was hydrothermally treated at 450 °C for 2 hours, loss of BET surface area and benzene adsorption capacity occurred. When MCM-41 was treated with 20% nitric acid overnight at room temperature, the BET surface area was slightly increased. It was associated with the removal of some blockages in MCM-41 channels. For 5% KOH solution, the MCM-41 structure was completely destructed.

Table 2.3 Thermal, hydrothermal and acid-base stability of MCM-41

Treatment method	XRD intensity	BET surface area	benzene uptake(%)
a) calcinations in N_2 at 540 °C for 1 h and then in air for 8 h, 1°C/min	100	1016	65.5
b) calcinations in air at 540 °C for 8 h, 1 °C/min	95	940	54.0
c) hydrothermally treated at 450 °C for 2 h	55	670	33.3
d) 20% nitric acid, room temperature, overnight	100	1114	65.5
e) 5% KOH solution, room temperature, overnight	0	3.5	0

2.4 Friedel-Craft Reactions[67]

In 1877 French chemists, Charles Friedel and James M. Crafts discovered new methods for preparing of alkylbenzenes (ArR) and acylbenzene (ArCOR). These reactions are now called Friedel-Crafts alkylation and acylation reactions. For Friedel-Crafts acylation, $AlCl_3$ removes chloride and forms acid chloride or acid anhydride, in order to generate acylium ions as electrophiles. After that, these electrophiles react with the reactant and produce desired products. Scheme 2.1 shows the reaction mechanism of Friedel-Crafts acylation. Notice that for the final step, $AlCl_3$ is consumed by adding water. Therefore, $Al(OH)_3$ and aromatic ketone are major products.

Step1: Electrophilic formation

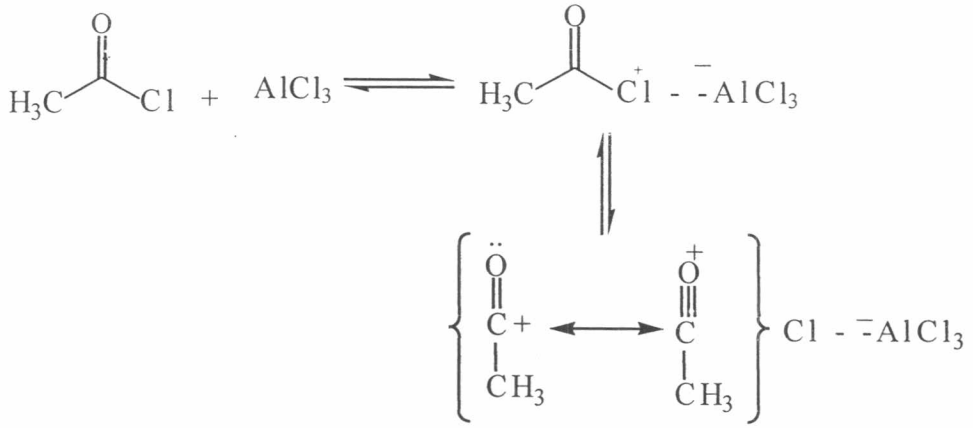

Step:2: Electrophilic substitution

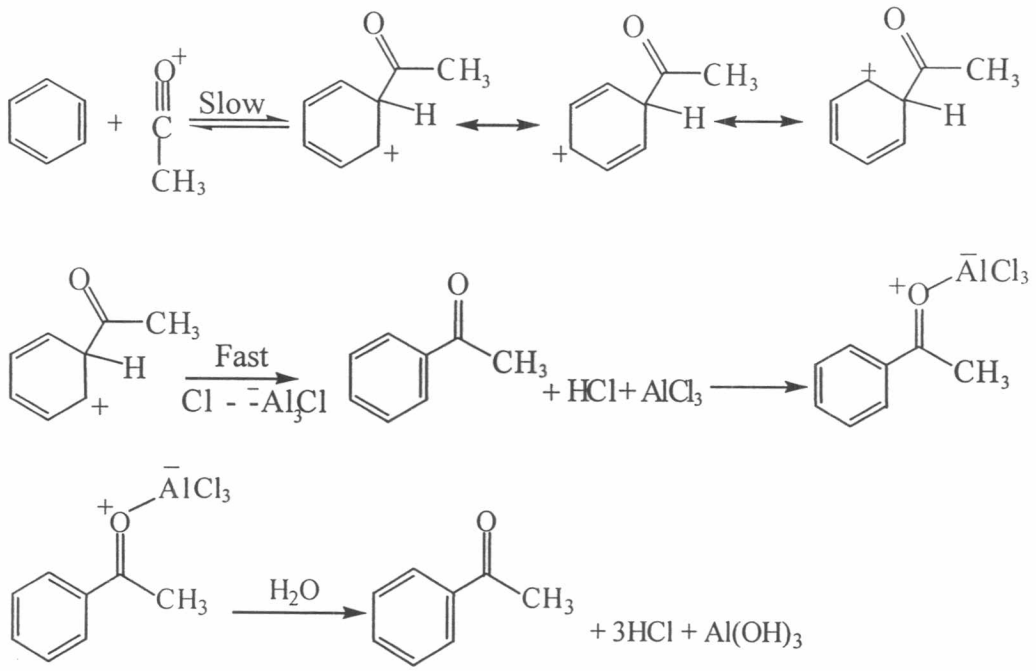

Scheme 2.1 Friedel-Crafts acylation mechamism

For Friedel-Crafts alkylation, carbocations are electrophiles. The reaction is performed with alkyl chloride and Lewis acid catalysts, e.g. $AlCl_3$ and $FeCl_3$. The catalyst forms the carbocation, which is easily attacked by benzene, as shown in Scheme 2.2

Step1: Electrophilic formation

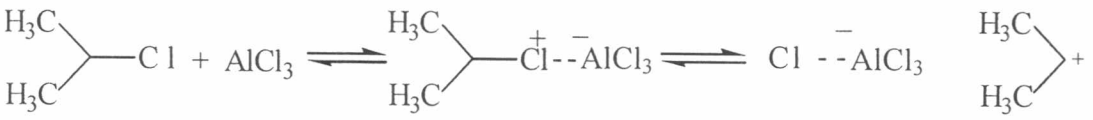

Step:2: Electrophilic substitution

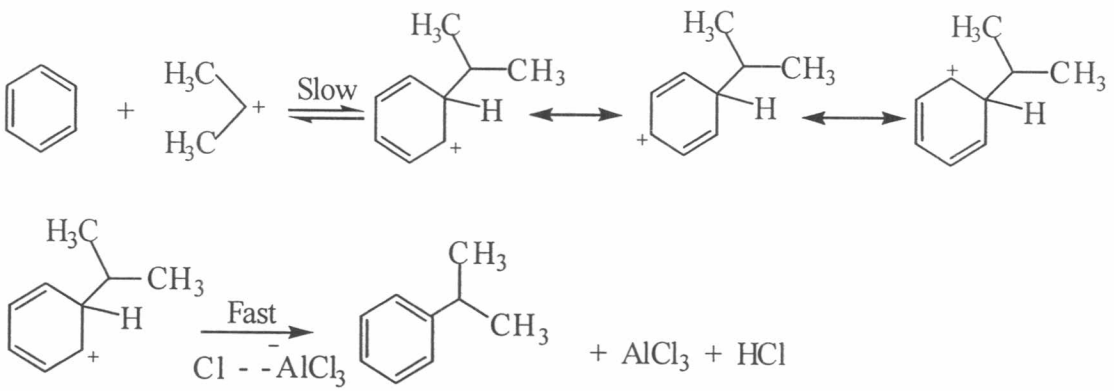

Scheme 2.2 Friedel-Crafts alkylation mechanism

Friedel-Crafts alkylations are not restricted to alkyl halides and aluminium chloride. Many reagents, which can form carbocation, may be used as well. These possibilities include a mixture of alkene and acid, and a mixture of alcohol and acid, as displayed in Scheme 2.3

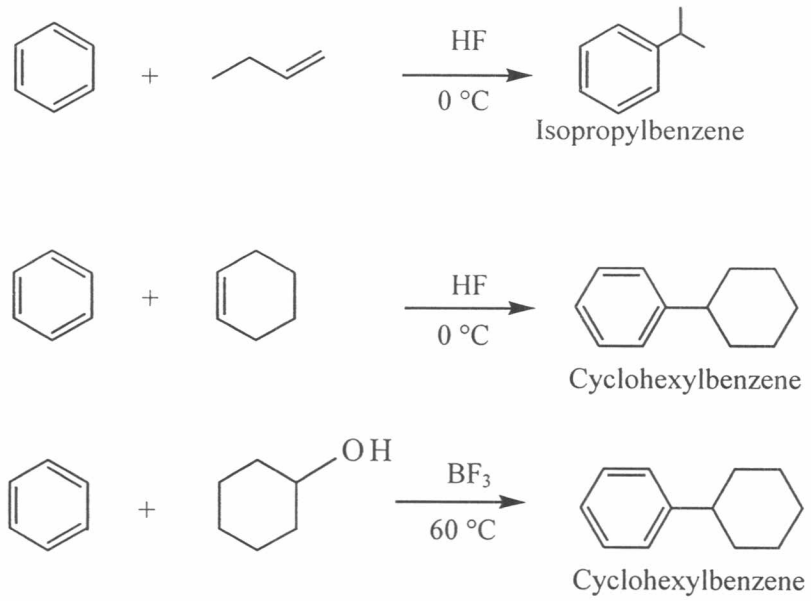

Scheme 2.3 Reagent pairs in Friedel-Crafts alkylation

Eventhough Friedel-Crafts reactions are well known and easily take place, there are some limitations as follows:

(1) The reaction between benzene and aryl halides or vinylic halides does not occur because the bond strength between carbon and halogen of a vinylic or phenyl halide is stronger than that of alkyl halide.

(2) The reactions do not work when electron withdrawing groups (EWG) such as $-NO_2$, -COOH, -CN, -C(O)R, and $-SO_3H$, are attached on the benzene ring, as shown in Scheme 2.4.

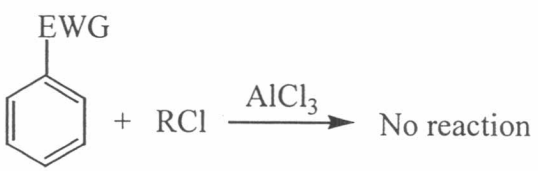

Scheme 2.4 Effect of electron withdrawing group on Friedel-Crafts alkylation

Scheme 2.5 displays the effect of amino groups, which well react with $AlCl_3$ and prohibit both acylation and alkylation reactions

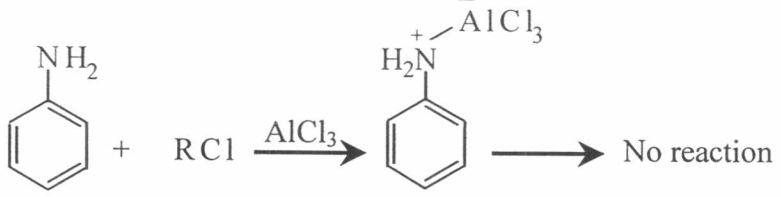

Scheme 2.5 Effect of amino group on Friedel-Crafts alkylation

(3) When carbocations are formed from alkyl halide, alkene, and alcohol, it can rearrange to more stable carbocation, as shown in Scheme 2.6, in the alkylation. No rearrangement occur during the acylation reaction.

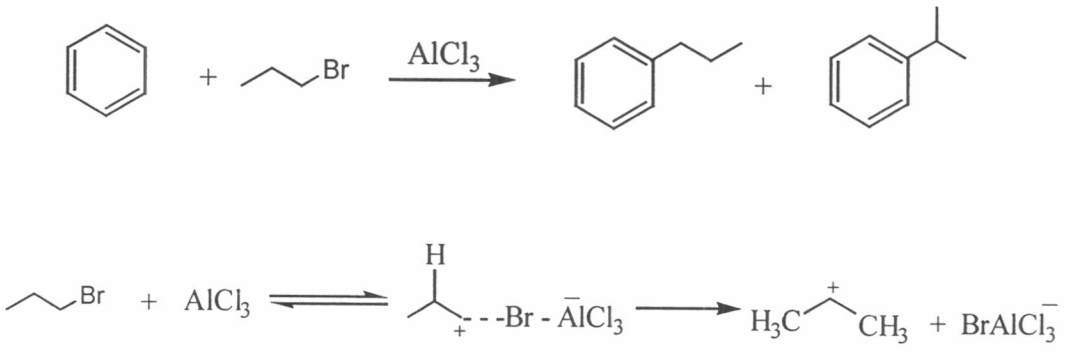

Scheme 2.6 Rearrangement of carbocation during alkylation reaction

(4) Polyalkylation can occur in Friedel-Crafts alkylation, as shown in Scheme 2.7, substituted benzene are more reactive and more electron rich than benzene itself.

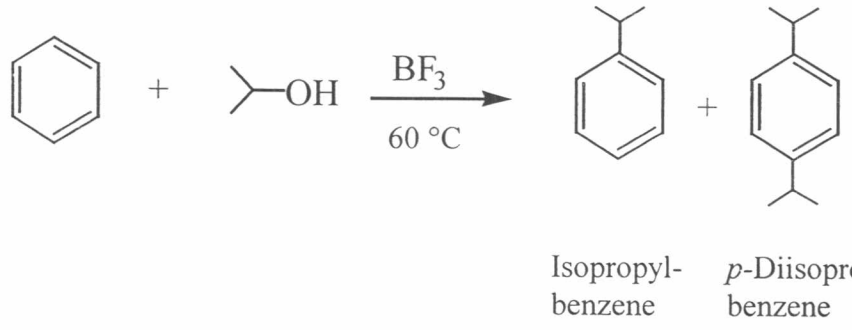

Scheme 2.7 Polyalkylation in Friedel-Crafts alkylation

In order to overcome the problems concerning rearrangement of carbocations and polyalkylation, the Wolff-Kishner reduction and Clemensen reduction have been suggested after the acylation step, as shown in Scheme 2.8. Therefore, the reduction yields only depend on alkyl benzene product from aromatic ketone.

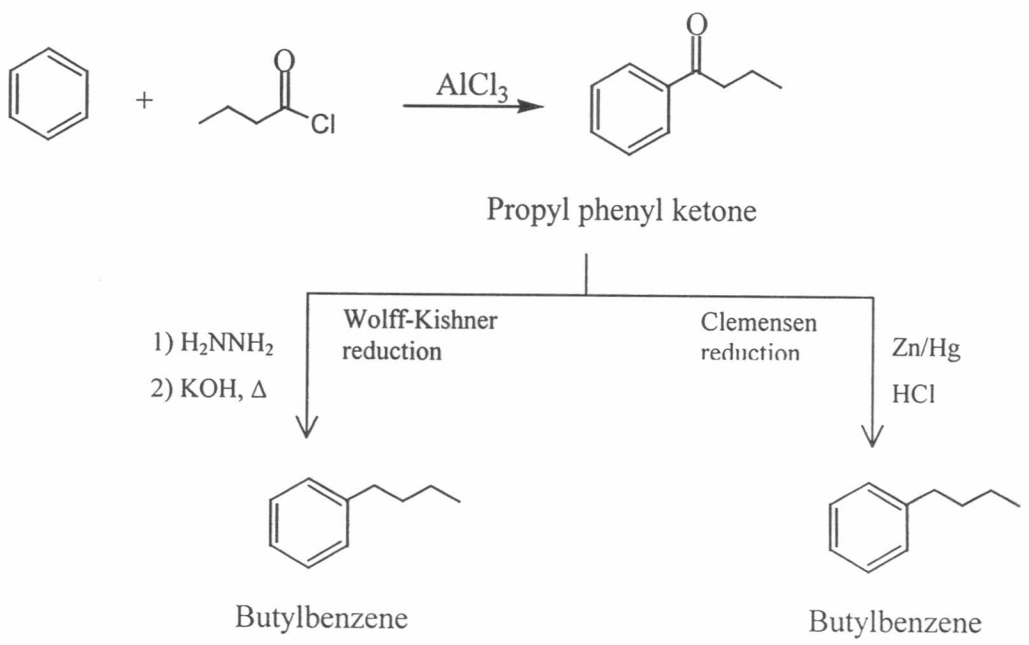

Scheme 2.8 Wolff-Kishner reduction and Clemensen reduction